J Shoulder Elbow Surg (2014) 23, 955-963

ELSEVIER

Journal of Shoulder and Elbow Surgery

www.elsevier.com/locate/ymse

Determination of humeral head size in anatomic shoulder replacement for glenohumeral osteoarthritis

Ari R. Youderian, MD[a,*], Eric T. Ricchetti, MD[b], Meghan Drews[b], Joseph P. Iannotti, MD, PhD[b,c]

[a]*Illinois Bone and Joint Institute, LLC, Morton Grove, IL, USA*
[b]*Department of Orthopaedic Surgery, Orthopaedic and Rheumatologic Institute, Cleveland Clinic, Cleveland, OH, USA*
[c]*Cleveland Clinic Lerner College of Medicine, Case Western Reserve University, Cleveland, OH, USA*

Background: We hypothesized that a sphere mapped to specific preserved nonarticular landmarks of the proximal humerus can accurately predict native humeral head radius of curvature (ROC) and head height (HH) in the osteoarthritic, deformed humeral head.

Methods: Three consistent nonarticular landmarks were defined with a 3-dimensional sphere (and 2-dimensional circle in midcoronal plane) placed along the articular surface in 31 normal cadaveric humeri. Side-to-side differences in ROC and HH were determined in 22 pairs of normal shoulders. Using the nonarticular landmarks and sphere method, 3 independent blinded observers performed 2 sets of measurements in 22 pairs of shoulders with unilateral glenohumeral osteoarthritis. The predicted native ROC and HH in the pathologic shoulder were compared with the normal side control.

Results: The mean side-to-side difference in normal shoulders was 0.2 mm (ROC) and 0.6 mm (HH). In the unilateral osteoarthritis cases, the intraobserver mean differences for the normal side were 0.3 mm (ROC) and 0.9 mm (HH). The pathologic side ROC and HH, defined by the sphere, exhibited intraobserver differences of 0.5 mm (ROC) and 1.0 mm (HH). The mean side-to-side differences between the normal and pathologic sides were 0.5 mm (ROC) with concordance correlation coefficient of 0.95 and 1.3 mm (HH) with concordance correlation coefficient of 0.66.

Conclusion: A sphere mapped to preserved nonarticular bone landmarks can be used for accurate preoperative measurement of premorbid humeral head size and therefore the selection of an anatomically sized prosthetic head. This is applicable postoperatively, as is a circle method for 2-dimensional assessment of anatomic humeral reconstruction in the coronal plane.

Level of evidence: Anatomy Study, Imaging.

Keywords: Anatomic shoulder replacement; humeral head size; glenohumeral arthritis; shoulder arthroplasty; preoperative planning; humerus templating; sphere model; 3D CT scan

IRB approval was obtained via Cleveland Clinic IRB #6235.
Funding for this project was provided by State of Ohio Biomedical Research and Development Fund.

*Reprint requests: Ari R. Youderian, MD, Illinois Bone and Joint Institute, LLC, 9000 Waukegan Road, Suite 200, Morton Grove, IL 60053, USA.
E-mail address: ayouderian@gmail.com (A.R. Youderian).

1058-2746/$ - see front matter © 2014 Journal of Shoulder and Elbow Surgery Board of Trustees.
http://dx.doi.org/10.1016/j.jse.2013.09.005

The native humeral head size is defined by the humeral head radius of curvature (ROC) and humeral head height (HH). Humeral HH is defined as the perpendicular linear distance from the anatomic neck to the apex of the humeral head. The humeral head is not a perfect sphere, and its ROC in the anteroposterior (AP) dimension (axial plane) is smaller than that of the superoinferior (SI) dimension (coronal plane), with an average ratio of 0.92.[3,9,15,16] In the setting of advanced glenohumeral osteoarthritis, the humeral head is deformed by loss of humeral HH and peripheral osteophytes, making it difficult to preoperatively define the anatomically correct prosthetic humeral head size. Moreover, a validated and reproducible method of determining a correctly sized and positioned prosthetic humeral head has not been presented. Preoperative implant templates are available, but a valid method for applying them to the preoperative radiographs to define anatomic head sizing or placement has not been validated. Most important, inaccurate selection of a prosthetic humeral head or position can result in overstuffing or undersizing of the reconstructed joint and can lead to poor outcomes, including shoulder stiffness, rotator cuff tearing, poor subscapularis tendon healing, and increased glenoid component wear or loosening and instability.[6,8,14,20-22]

Boileau and Walch described the relationship between the humeral head articular surface and the entire proximal humerus using a circle in the AP plane.[3] The authors reliably demonstrated that humeral head articular surface in the AP plane represented a circle in more than 88% of specimens and used this model to determine anterior-posterior offset from the humeral shaft to the center of rotation of the humeral head. These authors did not define the relationship of the humeral circle to the nonarticular surface landmarks of the proximal humerus.

We hypothesized that a three-dimensional (3D) sphere or a two-dimensional (2D) circle in the coronal plane of the humerus, superimposed on 3 specific landmarks of the nonarticular surface of the proximal humerus, would accurately predict humeral head ROC and HH in glenohumeral osteoarthritis. Together, these 2 measurements define the size of the articular portion of the humeral head and therefore the anatomically correct size of the prosthetic head.

Materials and methods

Overview of methods

The research consisted of 3 phases:

1. Definition of the relationship of a sphere (3D) and a circle (2D) placed onto the articular surface of the normal humeral head to determine the most consistent extra-articular bone landmarks that contacted either the sphere by 3D computed tomography (CT) or the circle on the midcoronal plane of the humerus. This was performed in scans of 31 unpaired cadaveric humeri.
2. Determination of the variability in side-to-side measurements of humeral head ROC, HH, and neck-shaft angle (NSA) in 22 pairs of normal shoulders.
3. Use of the sphere and circle method to determine the normal humeral head size from the pathologic condition in 22 pairs of shoulders with unilateral end-stage osteoarthritis. The method was validated by comparing the measured normal humeral head size in the pathologic shoulder with the measured head size in the patient's opposite normal shoulder.

Defining the spherical model

CT scans were performed on 31 normal unpaired cadaver humeri to define the relationship of the humeral articular surface to preserved landmarks of the proximal humerus and thereby to define a best fit sphere or circle model. These CT scans were generated from a randomly selected subset of normal cadaver specimens obtained from the Cleveland Museum of Natural History (Hamann-Todd Human Osteological Collection, Cleveland, OH, USA) with variable NSA measurements and were originally used for a previously published study at our institution.[10] Specimens were equal in number of males and females, ages 30 to 80 years, and free from traumatic or degenerative changes. Scans were performed with a 64-detector CT scanner (SOMATOM Sensation 64; Siemens Medical Solutions, Malvern, PA, USA) with 1-mm axial increments and a B60 reconstruction kernel.

By 3D CT simulation software (OrthoVis, Cleveland Clinic, Cleveland, OH, USA),[5-7,12,17-19] a digital sphere was best fit to the normal proximal humerus articular surface with both the 3D and 2D orthogonal images (Fig. 1). The sphere was matched to the central spherical articular surface of the humerus in both the midcoronal and midaxial planes. The humeral head is rarely a perfect sphere. In this study, the larger superior-inferior dimension defined in the midcoronal plane was used to determine the size of the sphere. The plane of the anatomic neck was defined by placing 3 points along the anatomic neck of the 3D image, superiorly, inferiorly, and anteriorly. The placement of the best fit sphere to the articular surface of the humeral head demonstrated 3 consistently preserved landmarks of the proximal humerus that would reliably confirm appropriate sizing and placement of the sphere: (1) the lateral cortex below the flare of the greater tuberosity, (2) the medial footprint of the rotator cuff on the greater tuberosity, and (3) the medial calcar at the anatomic neck (Fig. 1, *B*). The best fit sphere appears as a circle on the 2D images and follows the arc of curvature of the articular surface in the normal specimen. The midcoronal CT scan provides a 2D method for fitting of a circle and would correlate with a 2D anterior to posterior radiographic image of the proximal humerus.

HH was measured as the perpendicular distance from the anatomic neck plane to the apex of the sphere. This linear measurement was made on the 2D coronal image that captured the apex of the humeral head (Fig. 1, *B*). NSA was measured as the angle between the plane of the anatomic neck and the long axis of the humeral diaphysis, which was defined by a proximal and distal point in the center of the intramedullary canal (Fig. 2).

Determination of side-to-side variability using the sphere model on normal (paired) specimens

Side-to-side variations in ROC, HH, and NSA were measured in 22 pairs of normal shoulders (paired right and left sides), not used to develop the spherical model and its relationship with preserved proximal humeral landmarks, randomly selected from our CT

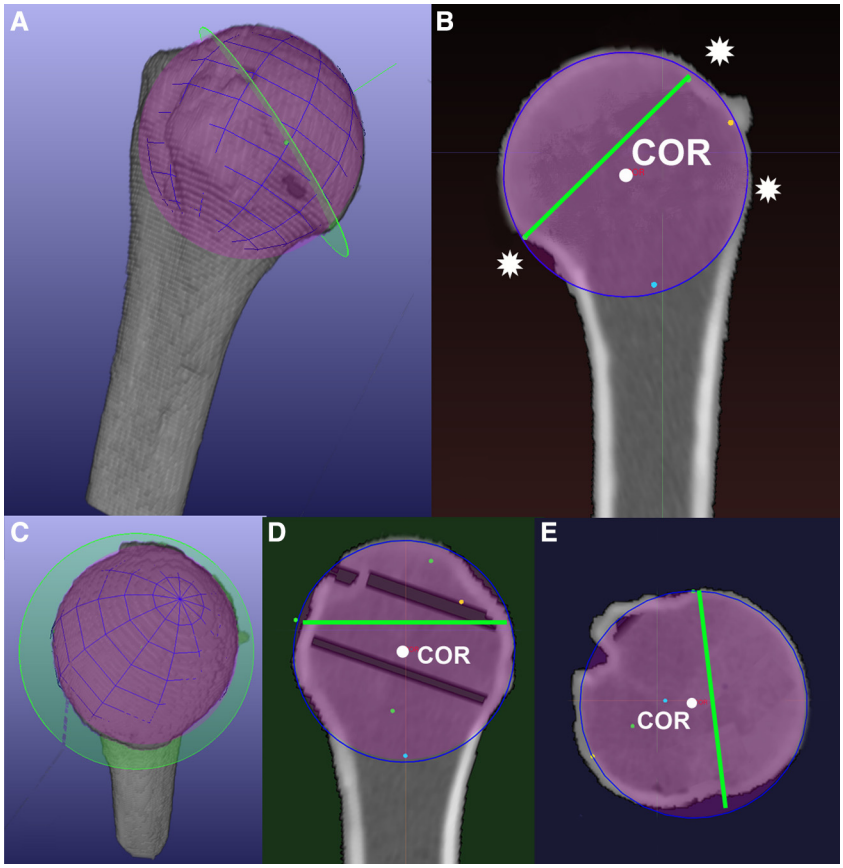

Figure 1 (**A-E**) Normal proximal humerus 3D CT, midcoronal, midsagittal, and midaxial 2D planes with sphere model *(purple),* anatomic neck *(green),* and center of rotation (COR, *white*). The commonly preserved nonarticular bone landmarks are noted in (**B**) with white stars.

image registry and reconstructed as 3D images. A single observer positioned and sized a digital sphere to align with the 3 preserved landmarks of the proximal humerus described before and, when possible, the articular surface in all 44 shoulders, thereby defining ROC for each specimen. The plane of the anatomic neck was defined as described before to determine HH and NSA.

Prediction of head size using the sphere and circle model in the pathologic humerus

Bilateral 3D CT scans were obtained from 22 patients with unilateral glenohumeral osteoarthritis who were scheduled for total shoulder arthroplasty. The contralateral, normal shoulder of each patient was used as the "gold standard" to define the accuracy of the sphere model to predict native humeral head measurements in the pathologic shoulder. The scans were de-identified before use, and no demographic data were available or associated with these scans. Each pair of scans was confirmed to have adequate image quality and the presence of primary osteoarthritis on one side with a normal-appearing shoulder on the opposite side. Scans were not included if there was any evidence of post-traumatic arthritis on the pathologic side.

Three observers with varying levels of clinical experience (one clinical shoulder fellow [A.R.Y.], one academic shoulder surgeon with 2+ years' experience [E.T.R.], and one academic shoulder surgeon with >20+ years' experience [J.P.I.]), performed 2 separate sets of measurements at least 2 weeks apart. Observers were blinded to their prior measurements made on the same or the opposite shoulder. Measurements of ROC, HH, and NSA were made in each shoulder as described in the previous section (Fig. 3). Intraobserver and interobserver differences in these measurements were calculated between all specimens and observers as well as between matched pairs of specimens. Differences in measurements of ROC, HH, and NSA between the normal and pathologic sides were used to determine the ability of the spherical model to predict native humeral head anatomy in the pathologic specimens. The mean differences, standard deviation, and range of measurements were calculated and compared.

Statistical analysis

For intraobserver comparisons, the mean difference (reading 1 − reading 2) and its 95% confidence interval (CI) were calculated overall and by observer to determine the variation between the 2 readings on the same measurement. This was performed for all 3 measurement variables (ROC, HH, and NSA). This was reported in both linear and absolute values.

The concordance correlation coefficient and 95% CI between the normal side reading and the pathologic side reading were calculated for each variable overall and by observer. For each specimen, the average of the 2 readings by each observer was taken to generate the final measurement for comparison. Scatter plots were also generated for overall agreement.

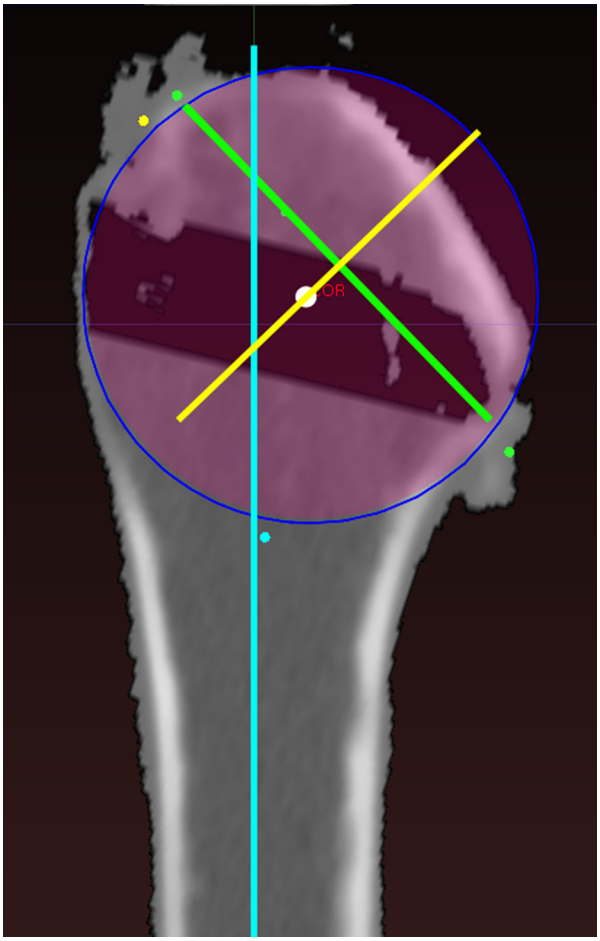

Figure 2 Neck-shaft angle (angle between yellow and blue lines) was determined in the 3D planning software by the angle between the intramedullary axis *(blue line)* and the perpendicular line *(yellow line)* to the anatomic neck plane *(green line)*.

Results

Normal specimens (paired): side-to-side variability

In the normal paired shoulders, the mean side-to-side (right to left) difference was 0.2 ± 0.2 mm (range, 0.0-0.8 mm) for ROC and 0.6 ± 0.4 mm (range, 0.1-1.4 mm) for humeral HH. The NSA demonstrated a side-to-side difference of 1.6° ± 1.3° (range, 0.1°-4.7°).

Unilateral osteoarthritis specimens (paired): intraobserver differences

In the unilateral osteoarthritis cases, the overall intraobserver mean difference for ROC between each measurement trial was 0.3 mm (95% CI, 0.3-0.4) for the normal side and 0.5 mm (95% CI, 0.4-0.6) for the pathologic side.

The intraobserver mean difference for humeral HH between each measurement trial was 0.9 mm (95% CI, 0.7-1.1) for the normal side and 1.0 mm (95% CI, 0.8-1.3) for the pathologic side.

The intraobserver mean difference for NSA between each measurement trial was 2.1° (95% CI, 1.6-2.6) for the normal side and 2.0° (95% CI, 1.5-2.5) for the pathologic side. The individual observer differences can be seen in Table I.

Unilateral osteoarthritis specimens (paired): side-to-side comparisons

The mean side-to-side difference in ROC between the normal and pathologic sides was 0.5 ± 0.4 mm (range, 0-1.9 mm) for all observers. The concordance correlation coefficients for ROC for each of the observers were 0.91, 0.98, and 0.95, respectively (Table II). The scatter plot demonstrated excellent overall agreement (Fig. 4, *A*).

The mean side-to-side difference for HH between the normal and pathologic sides was 1.3 ± 1.1 mm (range, 0.0-5.4 mm) for all observers. The concordance correlation coefficients for HH for each of the observers were 0.41, 0.89, and 0.68, respectively (Table II). The scatter plot demonstrated fair overall agreement (Fig. 4, *B*).

The mean side-to-side difference for NSA between the normal and pathologic sides was 1.8° ± 1.6° (range, 0.1°-10.3°) for all observers. The concordance correlation coefficients for NSA for each observer were 0.51, 0.43, and 0.34, respectively (Table II). The scatter plot demonstrated good overall agreement (Fig. 4, *C*).

Discussion

We have demonstrated that a sphere placed within the proximal humerus or a circle placed with use of the same landmarks on the midcoronal 2D plane can reliably define the premorbid humeral head size from the deformed proximal humerus in patients with advanced osteoarthritis. The average differences in ROC found between the normal controls and the pathologic specimens in all of our trials were commonly <0.5 mm, with excellent overall concordance correlation coefficient and agreement. This equates to a 1-mm difference in head size diameter. Given the sizing options of the current commercially available implants, these variations easily fit within these size options. We therefore believe that the variations in measurement between and within observers are clinically useful.

Lower correlations and agreement were found for the humeral HH and NSA measurements. However, the mean differences found between the pathologic and normal sides were still within 1 to 2 mm for HH and 1° to 3° for NSA. These measurement differences for HH fit within the range of the current commercially available anatomic component sizes for HH, which typically are offset by 3 mm. The actual prosthetic HH used at the time of surgery is likely to be more significantly affected by surgical variation in

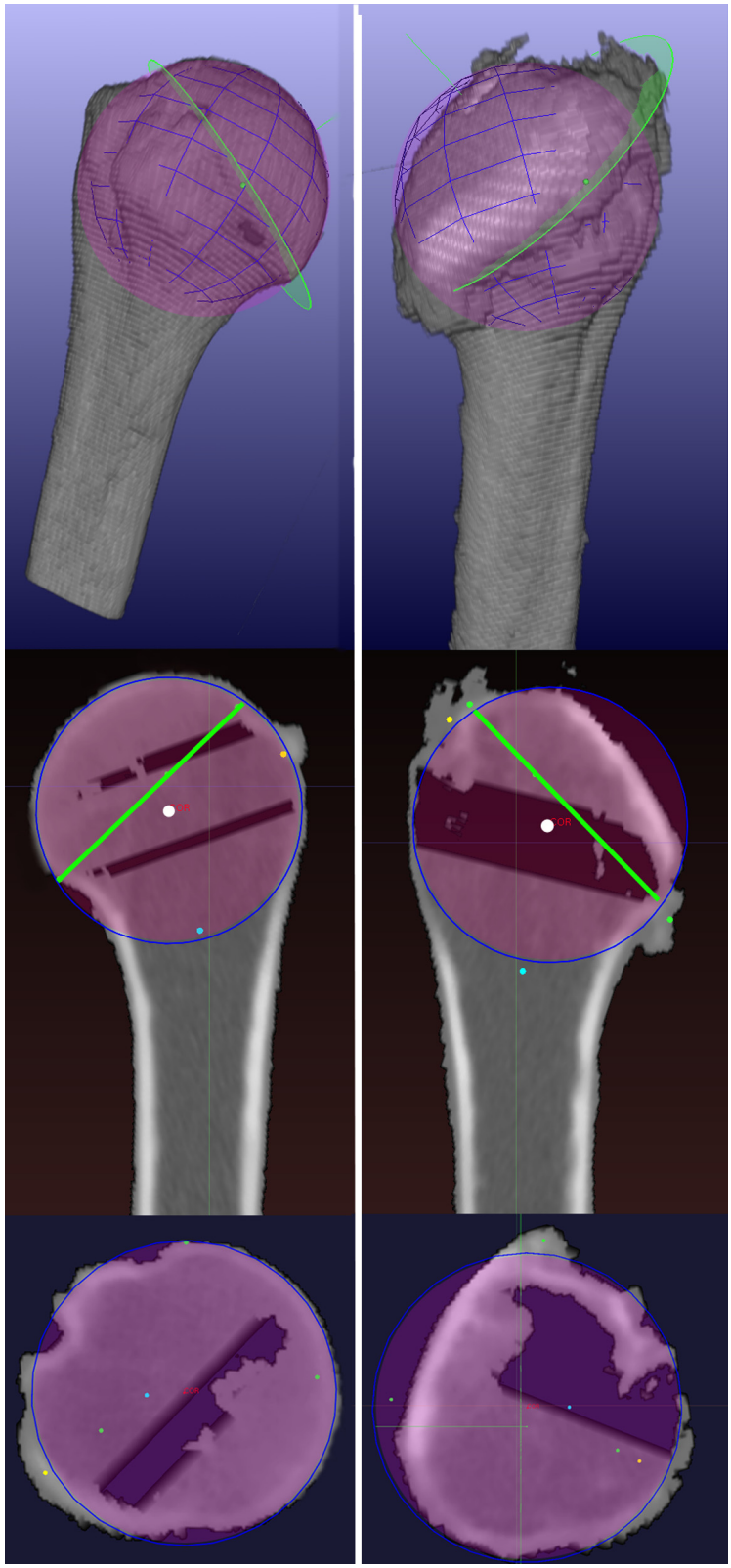

Figure 3 Side-to-side comparison in a patient with unilateral osteoarthritis. The best fit sphere is seen in purple with the anatomic neck *(green)* and center of rotation (COR, *white dot*).

Table I The mean difference of reading 1 and reading 2 and its 95% CI (absolute value)

	ROC	NSA	HH
Normal side			
Overall	0.3 (0.3, 0.4)	2.1 (1.6, 2.6)	0.9 (0.7, 1.1)
Observer 1	0.4 (0.2, 0.5)	1.1 (0.7, 1.5)	1.0 (0.6, 1.4)
Observer 2	0.3 (0.2, 0.4)	2.4 (1.6, 3.2)	0.6 (0.4, 0.8)
Observer 3	0.4 (0.2, 0.5)	2.9 (1.8, 4.0)	1.0 (0.6, 1.4)
Pathologic side			
Overall	0.5 (0.4, 0.6)	2.0 (1.5, 2.5)	1.0 (0.8, 1.3)
Observer 1	0.5 (0.3, 0.7)	1.5 (0.9, 2.0)	1.1 (0.7, 1.5)
Observer 2	0.3 (0.2, 0.4)	1.6 (0.8, 2.4)	0.8 (0.5, 1.1)
Observer 3	0.7 (0.4, 0.9)	3.0 (1.9, 4.0)	1.2 (0.7, 1.8)

HH, head height; *NSA*, neck-shaft angle; *ROC*, radius of curvature.

defining the anatomic neck and the ability of most surgeons to make an osteotomy exactly in the plane of the anatomic neck. We believe from our clinical experience that these variations in surgical technique that ultimately determine the prosthetic humeral HH used are within the range of 1- or 2-mm variation measured in this study.

The increased variability in measurement of humeral HH compared with the measurement of humeral head ROC is in part related to the methods used to define these variables in the current study. Whereas ROC is dependent only on best fit sphere placement, HH requires appropriate sphere placement as well as placement of the landmarks that define the anatomic neck plane. As defined before, the ROC can vary itself by an average of 0.5 mm, and the anatomic neck may also vary easily by 1 mm or 2° in either direction. Therefore, in any given patient, some of this variability in HH can be accounted for by the difference in both ROC and anatomic neck placement. The landmarks that define the anatomic neck are difficult to place in the software when there are large humeral osteophytes or significant bone loss. Defining the humeral anatomic neck at the time of surgery is also difficult for the same reasons.

We believe this new method for humeral head sizing is an improvement in both accuracy and concept over the few techniques that have previously been reported. Thinking of the entire proximal humerus as a sphere can help orthopaedic surgeons in all the stages of humeral head replacement, including preoperative planning, intraoperative decision-making, and postoperative assessment of the anatomic reconstruction of the shoulder. In the preoperative setting, extrapolation of this concept using a 2D circle on radiographs or 2D CT scans will be helpful in preoperative templating. This would require well-aligned, quality images and accounting for errors in magnification. Intraoperative sizing errors can probably be minimized by visualization of the trial implants in the coronal plane. A true coronal profile of the humeral head will form a circle that encompasses the lateral cortex and medial calcar (Fig. 5). In addition, this concept can be applied to postoperative radiographs by more accurately comparing the prosthetic humeral head center of rotation with the anatomic humeral head center of rotation. A simple circle, sized to the lateral cortex and medial calcar, on an internally rotated image (with the implant in profile) should align with the humeral head curvature (Fig. 6). Reasons for deviations in head size or position from this anatomic circle can then be determined by this method.

Table II Concordance correlation coefficient and 95% CI for the independent observer trials in paired unilateral osteoarthritis specimens

	Observer 1	Observer 2	Observer 3
ROC	0.91 (0.79, 0.96)	0.98 (0.96, 0.99)	0.95 (0.89, 0.98)
NSA	0.51 (0.13, 0.76)	0.43 (0.13, 0.67)	0.34 (0.01, 0.61)
HH	0.41 (0.11, 0.65)	0.89 (0.76, 0.96)	0.68 (0.40, 0.85)

HH, head height; *NSA*, neck-shaft angle; *ROC*, radius of curvature.

Although a specific head size can be determined accurately on preoperative imaging, the actual head size used is influenced by other surgical factors. Differences between planned and actual head size can occur by variability in the location of the osteotomy and defining the anatomic neck location or the angle of the osteotomy in relation to the humeral shaft. Nonanatomic prosthetic reconstruction can also be related to placing the correctly sized head in an incorrect position. Some deviation in the prosthetic humeral reconstruction may be intentional to compensate for soft tissue disease and to optimize prosthetic stability.

Applications of the 3D digital sphere model can be used for the 3D analysis of humeral alignment with the glenoid both preoperatively and postoperatively. The increased accuracy of this model to define the premorbid humeral center of rotation can then better assess the pathologic translation from the center of the glenoid or the scapular plane in both 2 dimensions and 3D space. The reproducibility and accuracy of the sphere method are likely to improve our ability to correlate clinical outcome and anatomic outcome.

The main disadvantage to the routine use of CT scans for preoperative planning in shoulder replacement is the inherent risk relating to radiation exposure and cost. The amount of radiation exposure of a shoulder CT scan has been reported to be approximately 2.06 mSv, less than the cumulative amount of natural radiation exposure in 1 calendar year.[1] The actual cost of a CT scan is extremely variable between institutions and states but probably ranges from hundreds to a few thousand dollars.[11] This information should be considered in making clinical decisions about the routine use of CT scans for preoperative planning, especially in patients with higher levels of previous radiation exposure. The advantages of preoperative CT scans for shoulder replacement are well established with both 2D and 3D imaging for assessment of the glenoid; increased accuracy and reliability in determining glenoid version and bone loss have both been demonstrated.[2,4,5,7,12,13,17,18] This study highlights the ability of preoperative CT scanning to provide valuable information specifically in regard to the

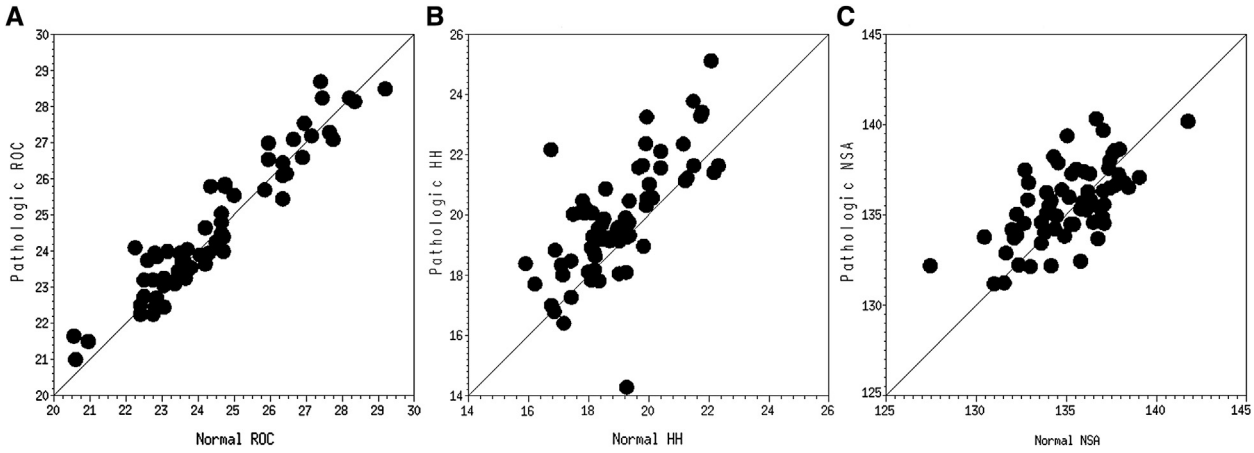

Figure 4 (**A-C**) Scatter plots for radius of curvature (ROC), head height (HH), and neck-shaft angle (NSA) comparing measurements between normal and pathologic sides.

humeral head component. Overstuffing of the humeral component can lead to limited range of motion, rotator cuff tears, eccentric or accelerated glenoid component wear, and poor function.[6,8,14,20-22] Therefore, the additional preoperative information gained by these methods may limit the amount of these errors that surgeons, both those experienced in shoulder replacements and generalists, may make. It is often easier to perform 3D imaging and templating of the humerus with the use of a sphere than at the time of surgery. The identification of bone landmarks and proper sizing are not limited by the soft tissue constraints and limited visualization found at the time of surgery.

The limitations of our study include the use of CT scans that do not account for native cartilage thickness. The articular cartilage of the humeral head has a uniform thickness and therefore the relationships defined in this study are likely to be maintained if the study were to be repeated by imaging studies that include the articular cartilage. The largest variation in measurements made in this model is the identification of the anatomic neck in the pathologic shoulder, thereby affecting the measurement of HH and NSA. The challenges in the assessment of the anatomic neck in the virtual software technique are also challenges during surgery with advanced deformity of the humeral head.

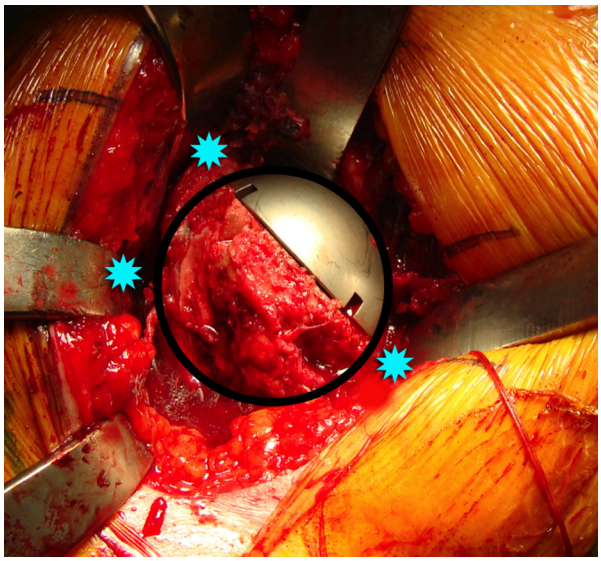

Figure 5 Intraoperative photograph of profiled proximal humerus demonstrating preserved landmarks *(stars)* and reconstruction with anatomic prosthetic head. On profile, the humeral head replacement should form a circle that includes the head, lateral cortex, and medial calcar.

Anatomic studies confirm that the humeral head geometry has a variable amount of sphericity,[3,9] especially as it is measured on the peripheral margins of the head. Current humeral head implants are completely spherical in both the AP and SI dimensions. Surgeons vary in their use of the AP or SI dimension for sizing of the humeral head at the time of surgery, and it is still unclear which provides the best clinical outcome. Our model uses the SI dimension preferentially with the understanding that there is possible oversizing by 2 to 4 mm in the AP dimension when a spherical prosthetic head is used. Nonetheless, 3D preoperative planning can easily demonstrate and predict this. The digital sphere can be sized by use of the AP dimension just as easily.

Finally, we do not discount the importance of intraoperative assessment and surgical skill to assess the entire shoulder in performing anatomic shoulder replacement. Proper balancing of the soft tissue envelope is critical to the success of shoulder replacement. Our method for sizing provides surgeons with information about the bone relationships. In our experience, this anatomic sizing of the humerus along with standard capsular releases and an intact rotator cuff provides excellent reliability to reproduce adequate soft tissue balance and subsequent range of motion and function in most cases. However, occasions arise that require deviations from a truly anatomically fixed humeral head, including but not limited to increased soft

Figure 6 Postoperative radiograph with proximal humeral replacement in profile demonstrating that a circle placed along the radius of curvature of the implant matches closely with the preserved bone landmarks.

tissue laxity, range of motion deficits, glenoid medialization, and hemiarthroplasty in the setting of cuff tear arthropathy.

Conclusions

We demonstrated and validate the concept that a sphere, superimposed on specific preserved extra-articular landmarks of the proximal humerus with use of 3D CT scans, or a circle in the midcoronal plane can be used to accurately predict humeral head size and HH in glenohumeral osteoarthritis. In this multiple-observer study, the humeral head ROC was predicted to within 0.5 ± 0.4 mm by these methods. The use of this simple, accurate method to determine humeral head size in the preoperative setting can help to more reliably restore native anatomic relationships in total shoulder arthroplasty, thereby avoiding potential clinical problems associated with poor humeral sizing. There is potential for this method also to be useful in postoperative shoulder replacement radiographic assessment and revision cases.

Disclaimer

Joseph P. Iannotti is a board member of the *Journal of Shoulder and Elbow Surgery* and is a paid consultant for DePuy, Tornier, and Zimmer. He has received grant funding from the State of Ohio Development Grant. He serves as a speaker for DePuy.

The other authors, their immediate families, and any research foundations with which they are affiliated have not received any financial payments or other benefits from any commercial entity related to the subject of this article.

References

1. Biswas D, Bible JE, Bohan M, Simpson AK, Whang PG, Grauer JN. Radiation exposure from musculoskeletal computed tomographic scans. J Bone Joint Surg Am 2009;91:1882-9. http://dx.doi.org/10.2106/JBJS.H.01199
2. Bokor DJ, O'Sullivan MD, Hazan GJ. Variability of measurement of glenoid version on computed tomography scan. J Shoulder Elbow Surg 1999;8:595-8.
3. Boileau P, Walch G. The three-dimensional geometry of the proximal humerus. Implications for surgical technique and prosthetic design. J Bone Joint Surg Br 1997;79:857-65.
4. Bryce CD, Davison AC, Lewis GS, Wang L, Flemming DJ, Armstrong AD. Two-dimensional glenoid version measurements vary with coronal and sagittal scapular rotation. J Bone Joint Surg Am 2010;92:692-9. http://dx.doi.org/10.2106/JBJS.I.00177
5. Codsi MJ, Bennetts C, Gordiev K, Boeck DM, Kwon Y, Brems J, et al. Normal glenoid vault anatomy and validation of a novel glenoid implant shape. J Shoulder Elbow Surg 2008;17:471-8. http://dx.doi.org/10.1016/j.jse.2007.08.010
6. Favre P, Moor B, Snedeker JG, Gerber C. Influence of component positioning on impingement in conventional total shoulder arthroplasty. Clin Biomech (Bristol, Avon) 2008;23:175-83. http://dx.doi.org/10.1016/j.clinbiomech.2007.09.009
7. Ganapathi A, McCarron JA, Chen X, Iannotti JP. Predicting normal glenoid version from the pathologic scapula: a comparison of 4 methods in 2- and 3-dimensional models. J Shoulder Elbow Surg 2011;20:234-44. http://dx.doi.org/10.1016/j.jse.2010.05.024
8. Harryman DT, Sidles JA, Harris SL, Lippitt SB, Matsen FA III. The effect of articular conformity and the size of the humeral head component on laxity and motion after glenohumeral arthroplasty. A study in cadavera. J Bone Joint Surg Am 1995;77:555-63.
9. Iannotti JP, Gabriel JP, Schneck SL, Evans BG, Misra S. The normal glenohumeral relationships. An anatomical study of one hundred and forty shoulders. J Bone Joint Surg Am 1992;74:491-500.
10. Jeong J, Bryan J, Iannotti JP. Effect of a variable prosthetic neck-shaft angle and the surgical technique on replication of normal humeral anatomy. J Bone Joint Surg Am 2009;91:1932-41. http://dx.doi.org/10.2106/JBJS.H.00729
11. Jones AC, Woldemikael D, Fisher T, Hobbs GR, Prud'homme BJ, Bal GK. Repeated computed tomographic scans in transferred trauma patients: indications, costs, and radiation exposure. Trauma Acute Care Surg 2012;73:1564-9. http://dx.doi.org/10.1097/TA.0b013e31826fc85f
12. Kwon YW, Powell KA, Yum JK, Brems JJ, Iannotti JP. Use of three-dimensional computed tomography for the analysis of the glenoid anatomy. J Shoulder Elbow Surg 2005;14:85-90. http://dx.doi.org/10.1016/j.jse.2004.04.011
13. Nyffeler RW, Jost B, Pfirrmann CW, Gerber C. Measurement of glenoid version: conventional radiographs versus computed tomography scans. J Shoulder Elbow Surg 2003;12:493-6. http://dx.doi.org/10.1016/S1058-2746(03)00181-2
14. Nyffeler RW, Sheikh R, Jacob HA, Gerber C. Influence of humeral prosthesis height on biomechanics of glenohumeral abduction. An in vitro study. J Bone Joint Surg Am 2004;86A:575-80.

15. Pearl ML. Proximal humeral anatomy in shoulder arthroplasty: implications for prosthetic design and surgical technique. J Shoulder Elbow Surg 2005;14(Suppl S):99S-104S. http://dx.doi.org/10.1016/j.jse.2004.09.025
16. Robertson DD, Yuan J, Bigliani LU, Flatow EL, Yamaguchi K. Three-dimensional analysis of the proximal part of the humerus: relevance to arthroplasty. J Bone Joint Surg Am 2000;82:1594-602.
17. Scalise JJ, Bryan J, Polster J, Brems JJ, Iannotti JP. Quantitative analysis of glenoid bone loss in osteoarthritis using three-dimensional computed tomography scans. J Shoulder Elbow Surg 2008;17:328-35. http://dx.doi.org/10.1016/j.jse.2007.07.013
18. Scalise JJ, Codsi MJ, Bryan J, Iannotti JP. The three-dimensional glenoid vault model can estimate normal glenoid version in osteoarthritis. J Shoulder Elbow Surg 2008;17:487-91. http://dx.doi.org/10.1016/j.jse.2007.09.006
19. Scalise JJ, Codsi MJ, Bryan J, Brems JJ, Iannotti JP. The influence of three-dimensional computed tomography images of the shoulder in preoperative planning for total shoulder arthroplasty. J Bone Joint Surg Am 2008;90:2438-45. http://dx.doi.org/10.2106/JBJS.G.01341
20. Terrier A, Ramondetti S, Merlini F, Piolettia DD, Farronb A. Biomechanical consequences of humeral component malpositioning after anatomical total shoulder arthroplasty. J Shoulder Elbow Surg 2010;19:1184-90. http://dx.doi.org/10.1016/j.jse.2010.06.006
21. Thomas SR, Sforza G, Levy O, Copeland SA. Geometrical analysis of Copeland surface replacement shoulder arthroplasty in relation to normal anatomy. J Shoulder Elbow Surg 2005;14:186-92. http://dx.doi.org/10.1016/j.jse.2004.06.013
22. Williams GR, Wong KL, Pepe MD, Tan V, Silverberg D, Ramsey ML, et al. The effect of articular malposition after total shoulder arthroplasty on glenohumeral translations, range of motion, and subacromial impingement. J Shoulder Elbow Surg 2001;10:399-409.